Journal of Design Intelligence
https://www.ffspub.com/index.php/jdi
ISSN 3104-9001 (print)
E-mail: jdi.office@ffspub.com

Article

Finite Element Simulation of Human Body and Cushioning Materials in Falls: For the Development of Skateboarding Protective Pants

Yue Ni[1,2,3], Zhaohui Wang[1,2,3,†]
[1] *College of Fashion and Design, Donghua University, Shanghai 200051, China*
[2] *Key Laboratory of Clothing Design & Technology, Ministry of Education, Donghua University, Shanghai 200051, China*
[3] *Shanghai Belt and Road Joint Laboratory of Textile Intelligent Manufacturing, Shanghai 200051, China*
[†] *E-mail: wzh_sh2007@dhu.edu.cn*

Received: February 28, 2026 / Revised: April 6, 2026 / Accepted: April 16, 2026 / Published online: April 24, 2026

Abstract: At present, the skateboard protective equipment on the market has many shortcomings: on the one hand, most of the protective equipment are independently worn, which are separated from trousers, which is not only inconvenient to wear, but also easy to shift during exercise; On the other hand, the selection of cushioning materials and thickness design of existing protective devices lack scientific analysis and rely more on experience, or the movement flexibility is affected by the thick and hard materials, so the balance of protection, flexibility and comfort cannot be achieved. Based on this, this study focused on the pain points of knee injury protection in skateboarding, and carried out the design research of protective skateboarding pants. Firstly, the finite element model of knee joint under three typical fall conditions, kneeling, lateral and prone, was constructed based on the THUMS manikin, and the stress distribution characteristics of knee joint bones under different impact speeds were revealed. Secondly, the quantitative relationship model between material thickness and stress attenuation is established through finite element simulation, and the high energy absorbing material and its optimal thickness configuration are selected. The results show that EVA material has the best stress attenuation effect; 9–12 mm is the best thickness range for both protection and comfort. Finally, a kind of protective skateboard pants with detachable panda pattern protector was developed. This research not only has practicability, but also can promote the interdisciplinary and integration, and provide new ideas and methods for the research of other sports protection, medical rehabilitation and safety fields, especially in the field of protective and functional clothing, such as racing clothes and extreme sports clothes, which has application prospects and innovation value.

Keywords: Finite Element Analysis; Knee Protector; Stress; Garment Design
https://doi.org/10.64509/jdi.12.79

1 Introduction

Skateboarding attracts a large number of teenagers and adults with its unique skills and challenges, but skateboarding is also accompanied by inherent risks that can not be ignored, which is a medium and high-risk sport. The high injury rate of skateboarding, especially among beginners, is more significant. Falling has become the most common injury inducement in skateboarding. Research shows that the incidence of sports injury of adolescent skateboarders is as high as 45.97%, and the injury mostly occurs in the early stage of practice. With the improvement of skateboarding skills, the injury rate will gradually decrease [1]. In addition, complex skills and high-altitude movements can also easily lead to skateboarders' injuries in sports, such as sprains, fractures, etc. during the Tokyo 2020 Summer Olympic Games, the incidence of injuries in skateboarding ranked fourth among all sports, and the incidence rate of injured athletes was 21 injuries per 100 athletes [2]. Therefore, how to integrate scientific and effective protective design into skatewear to reduce the risk of injury has become an important direction of skatewear design and research.

Based on a number of studies at home and abroad, the location of skateboarding injury presents diversified characteristics. Some scholars' studies show that the injury most

† Corresponding Author: Zhaohui Wang
*Academic Editor: Yan Hong

often occurs in the upper limb [3, 4], and some scholars have concluded that most of the injury occurs in the lower limb. Shi Feng [1] found through investigation that the proportion of knee injuries ranked first among adolescent skateboarding injuries, followed by wrists, fingers, elbows, hips and ankles. Yang Shun [5] focused his research on the fans of Urumqi Hello skateboard club and found that ankle injuries were the most common, followed by knee injuries. For professional skateboarders, the injury rate is generally high, and the forearm becomes one of the main parts of injury [6]. Tian Yang [7] and others used various research methods, such as literature, questionnaire survey and interview, to deeply analyze the sports injuries of skateboarders, and found that the ankle, knee, wrist and elbow were the main areas of sports injuries of skateboarders. Adrián Rodríguez-Rivadulla [8] and other scholars found that most injuries occurred in the lower limbs (69.7%), the most common injury site was the ankle (39.3%), followed by the knee (13.9%) and wrist/forearm (9.9%). In addition, the injury characteristics of different skateboard types are also different. Long board athletes are more prone to head and neck injuries, while standard skateboard athletes are mainly lower limb injuries [9]. In the children group, wrist is the most common injury site, while the incidence of head injury is low, but the consequences are more serious. 76.9% of head and face injuries are caused by skateboard falls [10, 11]. The injury risk of adolescent skateboarding is significantly higher than that of other groups [12], and most adolescent skaters will still choose to return to sports even if they experience serious injuries [13]. This phenomenon shows that the attraction of skateboarding may far outweigh the cost of injury.

Finite element analysis uses the method of mathematical approximation to simulate the real physical system. The complex continuous system is decomposed into a finite number of simple units by using simple and interactive elements to approximate the real system with a finite number of unknowns. The response of the whole system is simulated by analyzing the behavior of these units. Numerical simulation method has been applied to the research of impact protective clothing. Because of the high complexity of clothing modeling, researchers usually use the method of simplifying clothing to simulate. For example, Qiao Fangfang [14] and others simplified the human body as a backing material with regular geometry, and the stab resistant clothing as a three-dimensional entity with a certain thickness. Or simulate and analyze some simple clothes. Li J [15] and others built a finite element model based on the CT scan data of a Chinese elderly woman, and simulated the fall process at different speeds. By comparing the simulation results of wearing and not wearing safety vests, we can intuitively evaluate the effect of safety vests in reducing fall injuries. In addition, the finite element analysis method is also applicable to the bullet proof clothing [16]. By constructing the finite element model of the bullet proof clothing and simulating the bullet impact process, the dynamic response and protection effect of the bullet proof clothing when impacted by the bullet can be analyzed.

Because of its good flexibility and energy absorption, soft protective materials can effectively disperse the impact force, and are widely used in sports protective equipment, footwear and other fields. Common soft protective materials include EVA, P4U, Poron, etc. Polymer foams are widely used for energy absorption [17]. EVA (ethylene vinyl acetate copolymer) is a typical foam material, with excellent flexibility, elasticity and good impact protection and energy absorption performance [18], especially in low temperature environment, it can still maintain its energy absorption effect. Its unique structure enables it to absorb external impact through cell compression and expansion after stress. Because of its good elasticity and impact resistance [19], this material is widely used in shoe soles, sports mats, protective equipment and packaging materials. In recent years, the modification research of EVA material has made great progress. By adding modifiers such as foaming agent and plasticizer [20–22], its impact resistance and deformation recovery ability can be further optimized. P4U is an intelligent material independently developed by China. Its successful development not only fills the gap in the domestic market, but also breaks through international technical barriers, bringing innovative changes to the design and application of protective products. The material was developed by Shenzhen sur intelligent new material technology Co., Ltd. and was protected by the national invention patent. The inventor of P4U is Dr. Li Feng, associate professor of School of materials science and engineering, Xi'an University of technology and former senior scientist of mintek National Research Institute in South Africa. P4U is a non Newtonian fluid based on the shear thickening principle, similar to D3O [23]. P4U can be applied to the development of sports shoe sole material [24], which is soft and comfortable, with excellent cushioning and rebound performance. This material can also be made into composite foam material [25], which has excellent rigidity strength, wear resistance, antibacterial and deodorizing properties. Its unique functions expand the application scenarios of P4U from daily sports equipment to high-end protection and industrial fields. Poron, a kind of polyurethane foam in porous polymers, is a material with excellent cushioning properties. It has the characteristics of high density and excellent compression and deformation resistance, and can provide up to 7 times the impact protection effect compared with other materials [26]. At the same time, this material is very durable and not easy to age, so it has a wide range of applications and high cost performance, and can be used for various gasket materials. In recent years, Poron has been widely used in insoles [27–29] and has been proved to be the most effective shock absorption method.

Although the importance of reducing the risk of skateboarding injury has been recognized, the research on how to scientifically and effectively integrate protective design into skateboarding clothing is still not deep enough. Therefore, this research can promote the cross integration of materials science, computer science and other disciplines. This research not only has practicability, but also can promote the interdisciplinary and integration, and provide new ideas and methods for the research of other sports protection, medical rehabilitation and safety fields, especially in the field of protective and functional clothing, such as racing clothes and extreme sports clothes, which has application prospects and innovation value.

2 Method

2.1 Establishment of Fall Posture Model

2.1.1 Introduction of Finite Element Model

THUMS (Total Human Model for Safety) is a full manikin developed by Toyota Central Research Laboratory and Wayne State University [30]. The basic model used in this study is the THUMS 50th standing dummy (version 4.0), with a height of 175 cm and a weight of 77 kg. THUMS can simulate human injuries such as fracture, brain and visceral injury in collision. Although the physical crash dummy can simulate the collision process to a certain extent, it often focuses on the macro performance of the overall mechanical response, and the detailed analysis of the injury related to the collision is relatively limited, while the THUMS model can go deep into the micro level and analyze the injury caused by the collision in more detail by virtue of its accurately constructed human shape and scientifically set human durability parameters. THUMS has been continuously developed and improved for many times. Now it has derived many versions and types, covering models of different gender, age and physique, greatly expanding its scope of application. The latest model can accurately reproduce the shape and strength of the whole body including bones, brain, internal organs and muscles. THUMS has launched version 4.1 of AM50, AF05 and AM95 pedestrian models on June 30, 2025, and version 4.1 and 7 models of AM50 applicable to European NCAP technical bulletin CP550 v1.0 on January 23, 2026. The introduction of these new models will further enrich their application in the field of human safety research.

2.1.2 Skateboard Fall Posture Selection

Based on the field observation data, three typical fall postures, namely, kneeling posture, lateral posture and prone posture, were selected as the modeling postures. These three postures are the most common knee injury related postures in skateboarding in the field observation. Through the targeted analysis of the stress distribution of the bones of the knee joint under different fall conditions, it can better reflect the stress characteristics and injury risk of the knee joint under different fall scenarios. In the HyperMesh software, the upright THUMS 50th standing dummy (version 4.0) was preprocessed to adjust the mesh of joint parts to obtain different poses. The solver used LS-DYNA software, and the postprocessing used HyperWorks software. The built model is shown in Figure 1, Figure 2 and Figure 3.

2.2 Parameter Measurement and Model Establishment of Cushioning Materials

The mechanical properties of cushioning materials are the core factors that affect the impact protection effect of knee joint. Its density, elastic modulus and Poisson's ratio parameters directly determine the energy absorption and stress dispersion ability of materials under impact load. In this study, three typical buffer materials, namely polyurethane foam (Poron), ethylene vinyl acetate copolymer (EVA) and smart material (P4U), were selected, and their key mechanical parameters were obtained through standardized testing, and the finite element models of single-layer and multi-layer superposition were constructed.

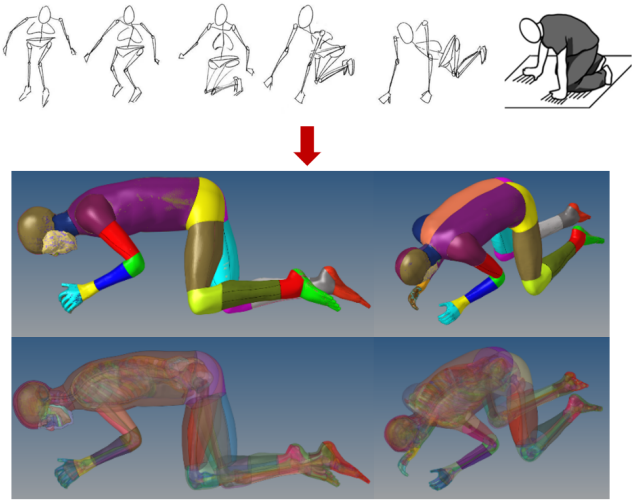

Figure 1: Comparison diagram of hand drawn modeling for kneeling and falling

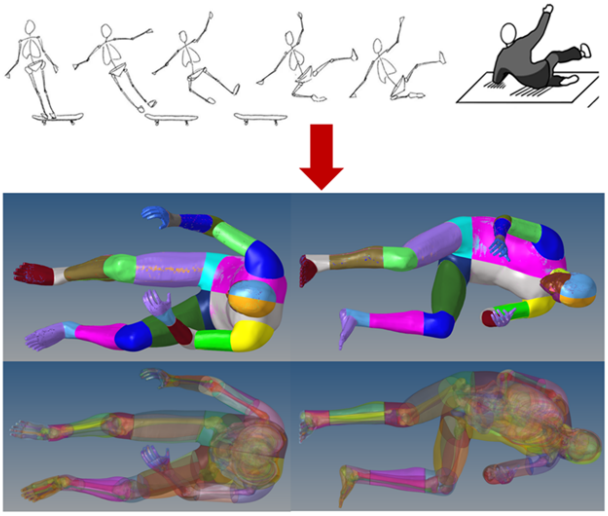

Figure 2: Comparison diagram of hand drawn modeling for side posture fall

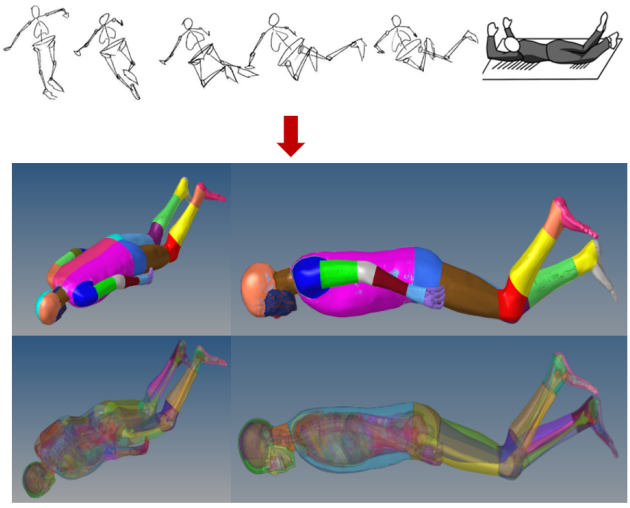

Figure 3: Comparison diagram of hand drawn modeling for falling in prone position

2.2.1 Density Test

Density test includes quality test and thickness test. The quality test is based on GB/T 26497-2022 electronic balance (replacing standard: GB/T 26497-2011). Three kinds of buffer materials with a thickness of about 0.3 cm are cut into a circle with a diameter of 58 mm. Six samples (numbered 1, 2, 3, 4, 5 and 6 respectively) are cut from each test material. A total of 18 samples are taken. When cutting, the distance from the edge of the material is at least 150 mm, and the parts with obvious defects such as folds and damages are avoided. The BSM-220.4 electronic balance is used. Each sample is tested for six times and the average value is taken. The thickness test is based on GB/T 3820-1997 textiles and textile products - Determination of thickness. The material is 18 samples cut during the quality test, using YG(B) 141D digital fabric thickness meter. Each sample is also tested for 6 times to take the average value. Through calculation, the density results are as follows: Poron is 0.2314 g/cm^3, EVA is 0.0667 g/cm^3, P4U is 0.2563 g/cm^3. Three samples are shown in Figure 4

Figure 4: The figure of the samples

2.2.2 Compression Modulus of Elasticity Test

The test basis for compressive modulus of elasticity is GB/T 8813-2020 determination of compressive properties of rigid cellular plastics. Prepare a 3 mm thick, flat and flawless specimen with a cutting size of 50*50 mm for each material, and test it with LE5105 electronic universal testing machine. Place the sample in the center between two parallel plates of the compression testing machine, compress the sample at the rate of 1mm/min, and record the force displacement curve. Within the proportional limit (i.e. in a linear relationship), the compressive stress is divided by its corresponding relative deformation. The compression modulus of elasticity E (MPa) finally measured Poron is 0.11476, EVA is 1.22785, P4U is 0.24923.

2.2.3 Poisson's Ratio Test

Poisson's ratio test is based on ASTM D 3575. Instron 68CS test instrument is used. The loading rate is 5mm/min. The transverse and longitudinal strains are monitored simultaneously by video extensometer, and the changes of load and displacement are recorded at the same time. Finally, the Poisson's ratio was 0.27 for Poron, 0.41 for EVA and 0.42 for P4U.

2.2.4 Buffer Material Modeling

In order to explore the impact of different cushioning materials on the knee joint protection of skateboarding, three kinds of cushioning material models with single layer of 3 mm and multi-layer superposition were constructed in this study. The model size was determined according to the knee joint protection area data, and the parameter assignment was completed based on the material mechanical property test results. Figure 5 and Figure 6 show two models of single layer 3 mm and five layers superimposed. Among them, the single-layer 3 mm model has a simple structure, which can directly reflect the basic cushioning performance of a single material. The five layer superposition model explores the composite effect of material superposition in impact protection through layer synergy.

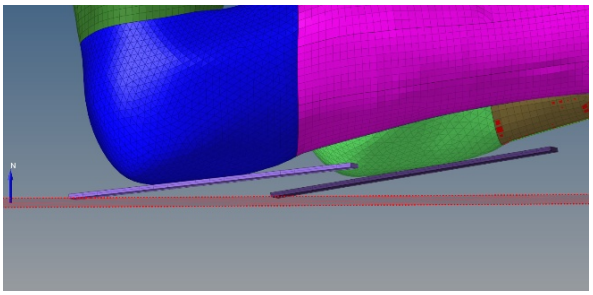

Figure 5: Single layer 3mm buffer material

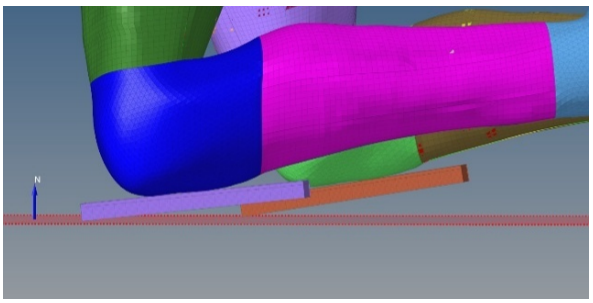

Figure 6: 5 layers of 3mm stacked buffer material

The key parameters of Poron, EVA and P4U are shown in Table 1:

Table 1: Buffer Material Assignment Table

Sample	Density (g/cm^3)	Compression modulus of elasticity (MPa)	Poisson's ratio
Poron	0.2314	0.11476	0.27
EVA	0.0667	1.22785	0.41
P4U	0.2563	0.24923	0.42

2.2.5 Material Model and Manikin Assembly

In order to systematically screen the optimal cushioning material and reasonable thickness for the knee joint protection of skateboard pants, it is necessary to carry out the assembly, simulation and comparative analysis of cushioning material model and manikin in two stages, taking into account the protection effect and human comfort. In the first stage, three kinds of buffer material models, Poron, EVA and P4U, were assembled with a uniform thickness of 15 mm. The stress attenuation effect of these models on the high stress bone of the knee joint was compared under the impact scene of 4 m/s kneeling posture, and the optimal material was selected; In the second stage, based on the optimal material, a multi thickness gradient of 3–15 mm was designed, and the protection effectiveness and realistic comfort requirements of different thickness were analyzed through assembly test to determine

the reasonable thickness parameters. Figure 7 is a simulation diagram of the assembly of the buffer material and the manikin, which visually shows the relative position and interaction between the buffer material and the manikin in the simulation environment.

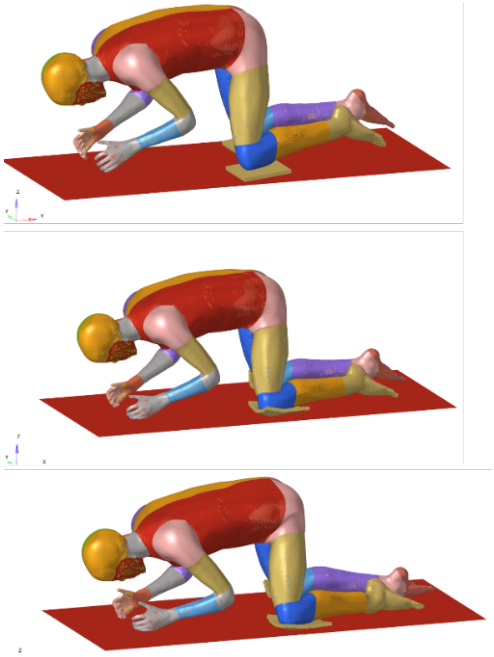

Figure 7: Simulation diagram of buffer material and manikin assembly

2.3 Impact Test Verification of Cushioning Materials

In order to verify the rationality of simulation, drop weight impact test was carried out to quantitatively evaluate the actual impact resistance of three kinds of buffer materials, and provide experimental data support for material selection. The test was conducted in accordance with ASTM D7136 Standard Test Method for measuring the damage resistance of fiber reinforced polymer matrix composites to drop impact events. Three kinds of materials with an area of 150*100 mm and a thickness of 3 mm were prepared. Each material was stacked in three layers to make the total thickness of 9 mm. Instron 9450 was used as the test instrument. During operation, set the impact speed of the falling hammer to 4 m/s, and take the average value of each material after three tests. The final peak impact force results of each material are shown in Table 2.

Table 2: Peak impact force table

Sample	Peak impact force/N			average value
	1	2	3	
Poron	180.309	183.647	187.241	183.732
EVA	369.785	376.459	366.435	370.893
P4U	256.737	278.164	271.566	268.822

The higher the peak impact force in the drop weight impact test, the more effective the material can undertake and disperse the load in the impact process. Therefore, according to the average value of the peak impact force, the impact resistance of the three materials from good to bad is: EVA material has the best impact resistance, followed by P4U material, and Poron material has relatively weak impact resistance. This result is consistent with the conclusion of "the stress attenuation effect of EVA material is the best" in the previous finite element simulation, which verifies the rationality of the simulation model.

3 Results and Discussion

3.1 Analysis of The Relationship between Maximum Stress and Falling Speed

In the scene of skateboarding falls, impact velocity is the core variable that affects the mechanical response of knee joint bones. In this study, finite element simulation was used to analyze the influence of impact velocity (1–5 m/s) on the maximum stress of femur, patella, tibia and fibula under three typical fall postures, including kneeling, lateral and prone postures, so as to provide a theoretical basis for the differential design of impact protective pants. Bone fracture is related to the ultimate stress level in the finite element model. For dense bone, the level is between 100 and 130 MPa. Through model simulation, the failure levels of dense bone and cancellous bone are close to 130 MPa and 50 MPa respectively [31]. Therefore, the stress level of 130 MPa is taken as the index value of failure risk: once the stress value reaches 130 MPa, it is considered that bone damage has occurred.

The THUMS V5.0 manikin is used to simulate the falling scenes of the skateboard in the kneeling position, side position and prone position. The equivalent speed is 4 m/s, and the dynamic behavior of the key time nodes in the falling process is intercepted. Figure 8, Figure 9 and Figure 10 are screenshots of falls in three postures of the THUMS model. Figure 11shows the stress of each bone in the left leg when falling in the kneeling position.

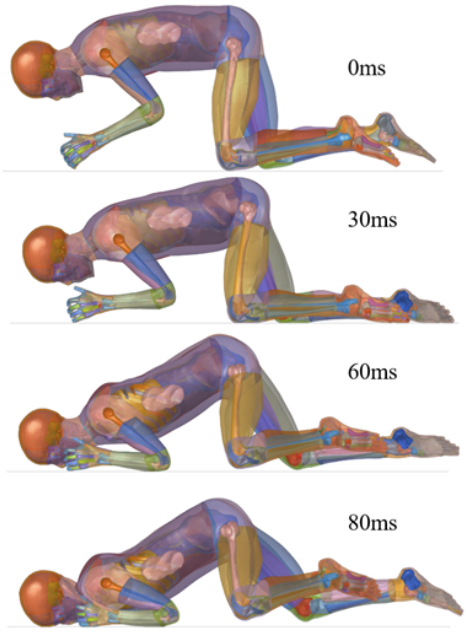

Figure 8: Kinematic behavior of the THUMS model when kneeling down on a rigid floor

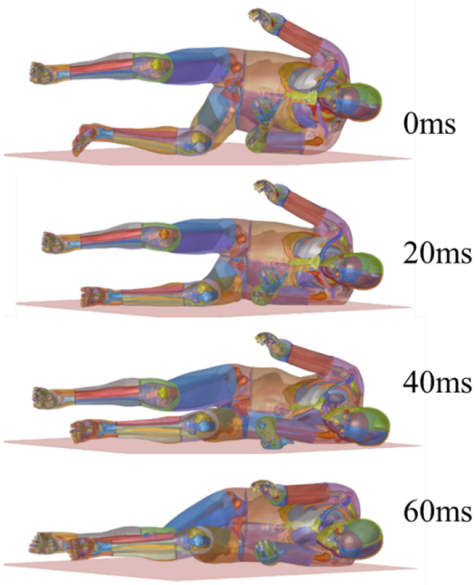

Figure 9: Kinematic behavior of THUMS model when falling on rigid floor with side posture

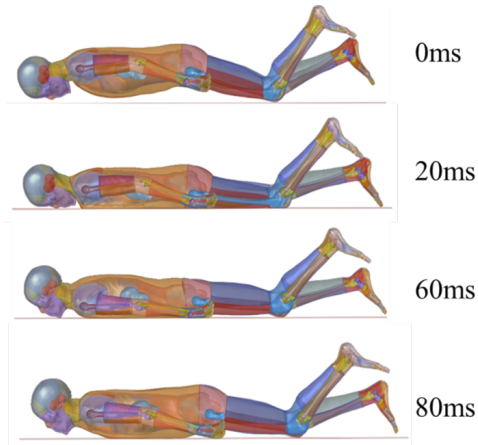

Figure 10: Kinematic behavior of THUMS model when falling on rigid floor in prone position

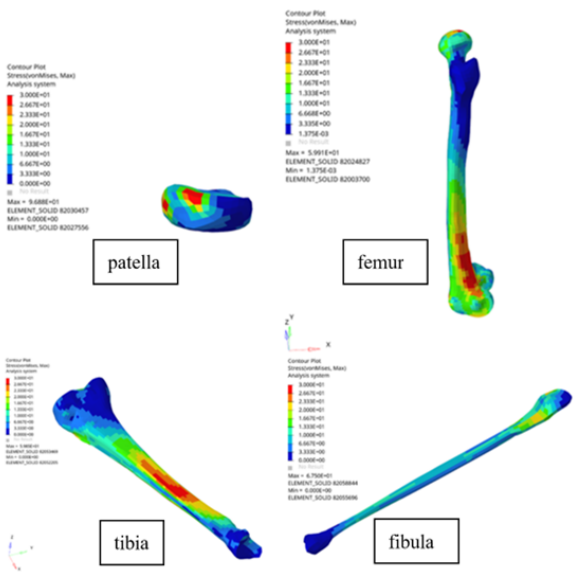

Figure 11: Stress diagram of left leg bones in kneeling position

3.1.1 Kneeling Posture

Through the analysis of the maximum stress data of the main bones (femur, patella, tibia, fibula) of the left and right legs at different impact speeds (1–5 m/s) when falling in the kneeling position, as shown in Figure 12 and Figure 13, the following conclusions can be drawn:

There was a significant positive correlation between the impact velocity and the maximum stress of bone: the maximum stress of all monitored bones increased continuously with the increase of impact velocity, no matter in the left or right leg. It shows that impact velocity is the key factor affecting the stress risk of bones, and the increase of velocity will significantly increase the load borne by bones. There are asymmetric differences in bone stress at the same part of the left and right legs: under the same impact speed, the maximum stress values of the corresponding bones of the left and right legs are not completely consistent, showing obvious asymmetry. This asymmetry may be related to the posture of the left and right legs when the human body falls in the kneeling position. Patella is the most stressed bone in kneeling fall: comparing the stress data of the bones of the left and right legs, the maximum stress of patella at the same speed is generally higher than that of other bones, and it is the core stress part in kneeling fall. The stress of the left patella at 4 m/s was 96.88 MPa, which was 1.62 times, 1.62 times and 1.44 times higher than that of the left femur (59.91 MPa), tibia (59.84

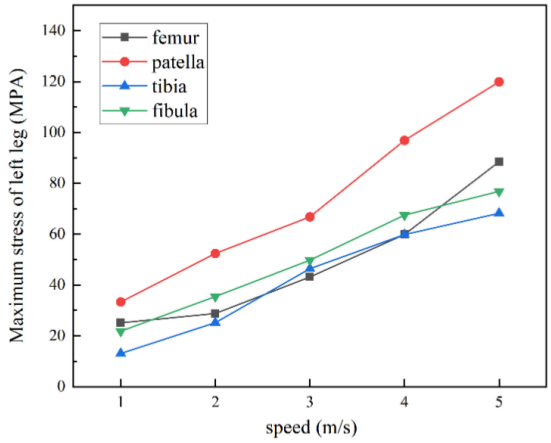

Figure 12: Broken line diagram of left leg kneeling fall speed and maximum bone stress

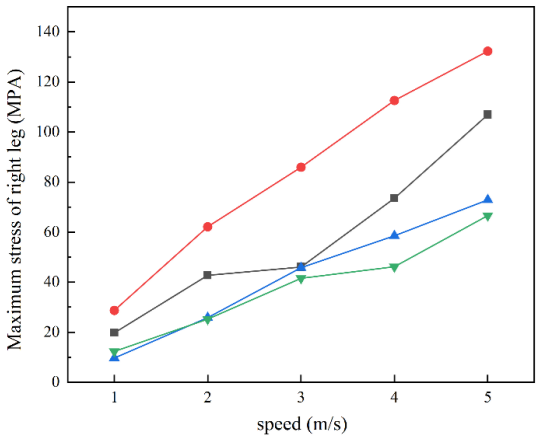

Figure 13: Broken line diagram of falling speed of right leg in kneeling position and maximum stress of bone

MPa) and fibula (67.50 MPa) at the same time; The stress of the right patella at 4 m/s was 112.60 MPa, which was 1.53 times, 1.92 times, and 2.44 times that of the femur (73.52 MPa), tibia (58.56 MPa), and fibula (46.20 MPa) of the right leg in the same period, indicating that the patella faced the highest stress risk in the kneeling posture fall scene, and was the focus of the protection design.

3.1.2 Side Posture (Left Leg Landing)

It is obviously different from the falling scene in the kneeling position. In the lateral position (left leg landing), although the maximum stress of the four bones of the left leg increases with the impact speed, the stress distribution of each bone is obviously differentiated, as shown in Figure 14. The stress of tibia increased most sharply, only 8.248 MPa at 1m/s, and 51.13 MPa at 5 m/s, with an increase of 519.9%; The stress of femur increased relatively gently, from 36.49 MPa to 57.81 MPa from 1 m/s to 5 m/s, with an increase of 58.4%; The stress of patella is always at a low level. This shows that in the side pose (left leg landing) scene, the sensitivity of different bones to speed changes varies greatly, and the tibia is the most sensitive force part to speed.

Different from the characteristics that the patella is the primary stress risk site when falling in the kneeling position, the left femur maintains the highest stress level at all speeds in the lateral position (left leg landing). The stress of 36.49 MPa at 1 m/s has far exceeded that of patella (3.292 MPa), tibia (8.248 MPa), fibula (11.92 MPa) at the same period, and the stress of 57.81MPa at 5m/S is still significantly higher than that of other bones. The patellar stress was the lowest at all speeds, only 3.292 MPa at 1m/s, which was less than 1/11 of the femoral stress at the same time. This change is due to the change of the stress transmission path of the left leg when the side posture falls. The lateral impact of the body is mainly carried by the femur, and the load of the patella is greatly reduced due to the deviation of the stress angle. Therefore, attention should also be paid to the lateral protection in the design of fall protection devices, and the dual protection of the femur and tibia should be paid at the same time to avoid the protection loopholes caused by ignoring the high-speed stress risk of the tibia.

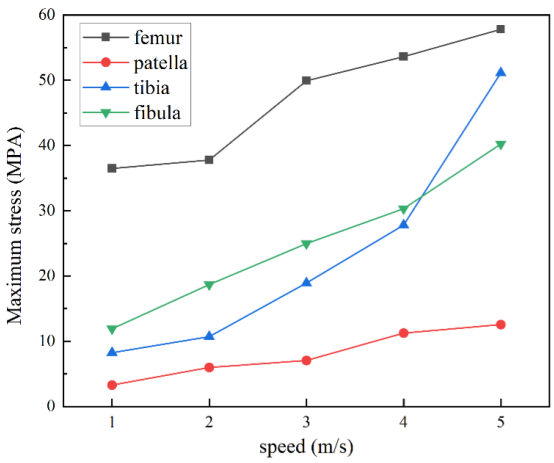

Figure 14: Broken line diagram of lateral fall speed and maximum stress of left leg bone

3.1.3 Prone Posture

By comparing the stress data of the bones of the left and right legs, it is clear that the maximum stress of the patella at all impact speeds is far higher than that of other bones in the same period, and it is the primary stress position when falling in the prone position, as shown in Figure 15 and Figure 16. In the left leg, the patella stress (28.06 MPa) at 1 m/s was 2.63 times that of the fibula (10.67 MPa) at the same time, and the patella stress (89.08 MPa) at 5 m/s was 1.85 times and 1.83 times that of the femur (48.18 MPa) and tibia (48.58 MPa) at the same time, respectively; The right leg was more extreme. At 2 m/s, the patella stress (55.05 MPa) was 3.87 times that of the fibula (14.22 MPa), and at 5 m/s, the patella stress (151.7 MPa) was 3.56 times that of the tibia (42.61 MPa) and 3.45 times that of the fibula (43.94 MPa). This series of data clearly shows that the stress risk of patella in the prone fall scene is much higher than that of other bones, and it is the key area that must be given priority in the protection design.

Except for patella, the stress levels of femur and tibia are relatively close, and keep a steady growth trend with the increase of impact velocity. In contrast, the fibula is at the lowest stress level, and the stress of left and right leg fibula does not exceed 45 MPa at 5 m/s.

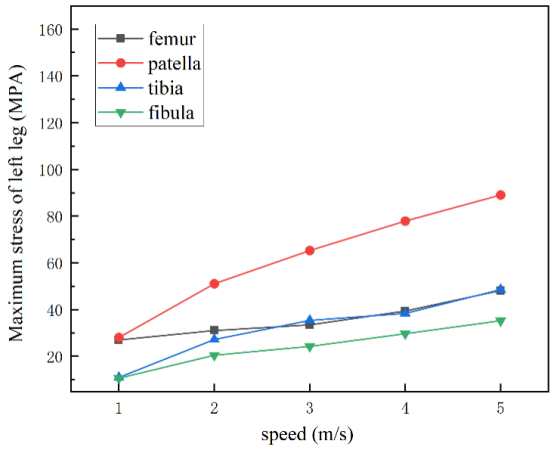

Figure 15: Broken line diagram of left leg falling speed and maximum bone stress

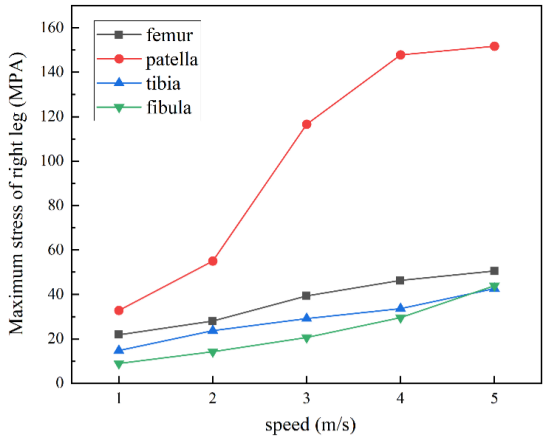

Figure 16: Broken line diagram of falling speed of right leg in prone position and maximum stress of bone

There is obvious asymmetry in the stress on the same part of the left and right legs, and the risk of patella in the right leg is prominent. At the same impact velocity, the maximum stress values of the corresponding bones of the left and right legs are significantly different. This asymmetry is speculated to be related to the deviation of body center of gravity and the sequence of leg contact with the ground at the moment of falling in prone position.

3.2 Analysis of Simulation Results and Selection of Cushioning Materials

3.2.1 Material Type Selection

Based on the 4 m/s kneeling and falling scene, the stress data of the knee joint bones in the ”unprotected” state were compared with the 15 mm thick Poron, EVA and P4U cushioning materials. The results are shown in Figure 17 and Figure 18.

Three kinds of materials can achieve stress attenuation, but EVA material has the best overall attenuation effect. Compared with the ”unprotected” state, the maximum stress of the three cushioning materials on the bones of the left and right legs were attenuated to varying degrees, and the attenuation amplitude of EVA material in all bone parts was significantly higher than that of Poron and P4U, showing a better overall protective effect.

Specifically, the attenuation performance of EVA material: the attenuation amplitude of EVA material on the patella of the left leg was the largest, from 96.88 MPa to 60.86 MPa, with an attenuation of 37.2%; The second was the femur of the left leg (from 59.91 MPa to 44.72 MPa, attenuation of 25.4%), the tibia of the left leg (from 59.85 MPa to 51.48 MPa, attenuation of 14.0%), and the fibula of the left leg (from 67.50 MPa to 61.43 MPa, attenuation of 8.9%). The attenuation performance of the right leg: the attenuation of EVA on the patella of the right leg was also the most prominent, from 112.6 MPa to 73.59 MPa, with an attenuation of 34.6%; The femur of the right leg decreased from 73.52 MPa to 49.74 MPa, with an attenuation of 32.3%; The tibia of the right leg decreased from 58.56 MPa to 45.65 MPa, with an attenuation of 22.0%; The fibula of the right leg decreased from 46.20 MPa to 40.74 MPa, with an attenuation of 11.8%. The attenuation amplitude of Poron and P4U were both lower than that of EVA: the attenuation of Poron on the left and right patella was only 6.4%–6.7%, while the attenuation of P4U on the left patella was 23.4%, and the attenuation of P4U on the right patella was 9.8%, which were far less than the protective effect of EVA.

Secondly, EVA has stronger pertinence to the attenuation of high stress bones, while Poron and P4U have obvious shortcomings in the protection of high stress parts. The attenuation amplitude of EVA for the patella of the left and right legs (34.6%–37.2%) was significantly higher than that for the fibula (8.9%–11.8%), which achieved the effect of ”key protection for high stress parts”.

Considering the overall attenuation effect of the three materials under the 15 mm thickness, EVA is the best buffer material under the 4 m/s kneeling fall scene. It can not only achieve the effective stress attenuation of various bone parts, but also achieve a significant reduction of more than 34.6% for the core risk point of kneeling fall (patella), which is significantly better than Poron and P4U, and can be used as the core material for the subsequent comparison of protection effects of different thicknesses.

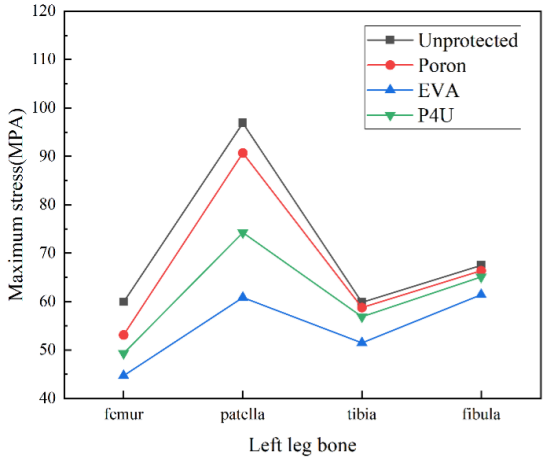

Figure 17: Maximum stress diagram of femur of left leg under protection of different materials

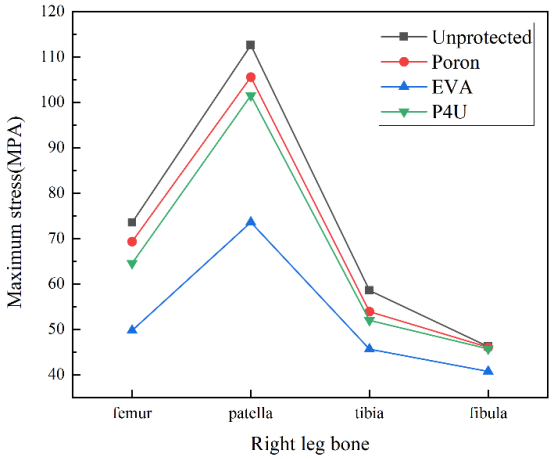

Figure 18: Maximum stress diagram of right femur under different material protection

3.2.2 Material Thickness Selection

Based on the 4 m/s kneeling and falling scene, the simulation model of EVA material with different thickness (3–15 mm) and the maximum stress of the bones (femur, patella, tibia, fibula) of the left and right knee joints was built. Combined with the benchmark data in the ”unprotected” state, the core law of stress variation with material thickness could be extracted to provide a quantitative basis for thickness optimization. The maximum stress results are shown in Figure 19 and Figure 20, and the specific analysis is as follows:

Overall rule: the stress decreases rapidly at first and then tends to be flat with the increase of material thickness. No matter in the left leg or the right leg, the maximum stress of each bone decreases with the increase of EVA material thickness, but there are significant differences in the stress decay rate between different thickness regions. The overall characteristics are ”rapid attenuation when the thickness is ≤ 9 mm, and slow attenuation when the thickness is > 9 mm”, and this trend is more obvious in high stress bones (patella, femur). The stress of the patella of the left leg decreased from 96.88 MPa to 88.57 MPa (8.6% reduction) when the thickness of

protection was 3 mm, to 77.82 MPa (12.1% reduction compared with 3 mm) when the thickness of protection was 6 mm, and to 68.30 MPa (12.2% reduction compared with 6 mm) when the thickness of protection was 9 mm; However, the attenuation of 12 mm is only 8.4% lower than that of 9 mm, and that of 15 mm is only 2.9% lower than that of 12 mm. When the right patella was protected with 3 mm thickness, the stress decreased from 112.6 MPa to 101.84 MPa (attenuation of 9.6%), 6 mm to 87.74 MPa (attenuation of 13.8% compared with 3 mm), 9 mm to 77.64MPa (attenuation of 11.5% compared with 6 mm); The attenuation rate of 12 mm is 4.0% lower than that of 9 mm, and that of 15 mm is 1.3% lower than that of 12 mm. The attenuation rate of 9 mm is significantly lower than that of 3–6 mm. This rule stems from the fact that there may be a threshold value for the absorption capacity of impact energy with the increase of material thickness. When the thickness is small, the deformation space of the material is limited, and increasing the thickness can significantly improve the energy absorption efficiency. When the thickness reaches a certain value (about 9 mm), the material can fully absorb most of the impact energy, and the increasing effect of continuous thickening on the energy absorption effect is not obvious, so the stress attenuation tends to be gentle.

Location difference: high stress bones are more sensitive to thickness changes, while low stress bones are less sensitive. The stress responses of different bones to material thickness changes were significantly different. The stress attenuation of patella and femur (high stress bones) was more sensitive to thickness changes, while tibia and fibula (low stress bones) were less sensitive. The specific performance was as follows: the cumulative stress attenuation of the left patella in the range of 3–9 mm was 29.5%, which was 3.9 times that of fibula (7.6%) in the same period; The cumulative stress attenuation of the right patella in the range of 3–9 mm was 31.0%, which was 2.8 times that of the tibia (11.1%) in the same period. The tibia and fibula of the left leg were attenuated by 14.0% and 9.0%, respectively; The tibia and fibula of the right leg were attenuated by 22.0% and 11.8% in the whole process, and there was no obvious attenuation after 9 mm, indicating that the demand for thickness change of low stress bones is low, and the protection effect of excessive thickening is limited.

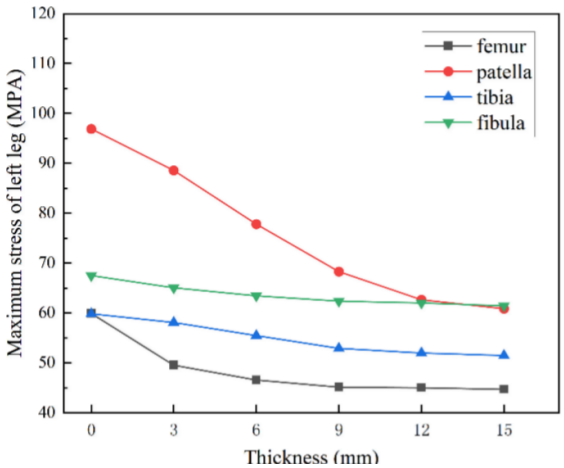

Figure 19: Maximum stress diagram of left leg under protection of EVA material with different thickness

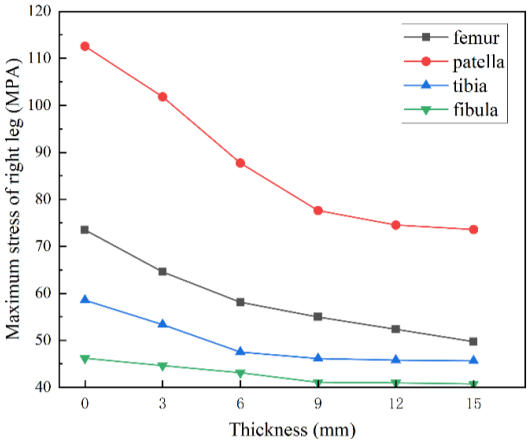

Figure 20: Maximum stress diagram of right leg under protection of EVA material with different thickness

Combined with the law of stress attenuation, and taking into account the overstaffing of trousers, sports restraint (comfort) and cost problems that may be caused by the increase of material thickness, 9mm thickness has been able to achieve a significant attenuation of high stress bones, and the attenuation amplitude of 12–15mm is less than 6%. The protection improvement is limited, which affects sports flexibility and comfort. The reasonable thickness range can be determined: 9–12mm is the optimal range for both protection and comfort.

3.3 Development of Skateboard Protective Pants

3.3.1 Design Description of Skateboard Protective Pants

The overall pants are loose fit. The loose fit can provide skateboarders with more free and comfortable wearing space, reduce the sense of bondage in the process of sports, and also conform to the current trend of leisure and fashion. Pleats are added at the knee to fit the situation of skateboarding with multi bending knee posture, and ensure that the knee can still maintain a comfortable activity state after the protective device is installed, and the smoothness and flexibility of the movement will not be affected too much due to the existence of the protective device. Field observation shows that more skateboarders tend to wear pants or even floor length pants, and the length of pants is designed as the length of the foot. The type of trouser leg is micro notched. During sports, the micro notched trouser leg can closely fit the ankle, effectively preventing the trouser leg from fluttering with the wind or interfering with the skateboard movement due to excessive movement range, avoiding the danger caused by the trouser leg involved in the skateboard wheel and other parts, ensuring the safety of skateboarders. Practical pockets are designed on both sides of trousers to meet the needs of skateboarders to place small items, such as mobile phones, keys, etc. Deep pocket capacity prevents items from falling during movement. The style design of skateboard protective pants is shown in Figure 21.

3.3.2 Design of Skateboard Protector

Appearance design of knee pads: skateboarding has both street trend and adventurous spirit, while panda, as a symbol of Chinese culture, represents a charmingly naive affinity and tenacious vitality. At the same time, the black and white color

Figure 21: Style drawing of skateboard protective pants

matching of panda is also in line with the color design of skateboarding pants. This time, the knee protection part of skateboarding pants selects the appearance of panda, which is to combine the local cultural symbols with the sports protection needs, and use the cultural enabling products to make the protective equipment break through the functional limitations, become the carrier of cultural identity and personality expression, and actively respond to the demands of skateboarding groups for unique style. Soft and energy absorbing materials are preferred for the protective equipment to ensure that the impact force can be effectively buffered during the movement, while ensuring the comfort of wearing and not affecting the flexibility of skateboarders. Combined with the simulation in the fourth chapter, EVA material is selected as the filling material of protective equipment.

Detachable design: the details of skateboard pants are shown in Figure 22. The protector at the knee is connected with the pants by zipper, which is convenient for the removal and installation of the protector, and the operation is convenient and efficient. The black-and-white color matching of panda protector and skateboarding pants are perfectly integrated to enhance the overall visual coordination. The protective device is made of nylon elastic fabric wrapped with EVA material, with seams left. The thickness of the inner buffer material can be increased or decreased freely according to the personal demand for protection degree, which not only meets the differential demand for protection under different skateboard scenes, but also provides users with personalized adjustment space, further improving the practicability and adaptability of the protective device.

Figure 22: Skate pants detail design

3.3.3 Skateboard Protective Pants Exhibition

The removable protector is shown in Figure 23. The finished skateboard pants are shown in Figure 24.

Figure 23: Detail drawing of removable protector

Figure 24: Finished skateboard pants

3.3.4 Performance Evaluation of Skateboard Protective Pants

In order to make the performance evaluation results closer to reality, this study developed an outdoor subjective evaluation experiment for skateboarders. Twenty healthy subjects (10 males and 10 females) were selected for the experiment. The average age, height and weight of all subjects are shown in Table 3. BMI values are at normal levels. Subjects should avoid strenuous exercise and maintain a stable state of mind before the experiment.

Table 3: Subject information

	Age	Height (cm)	Weight (kg)	BMI (kg/m^2)
Male average	23.25	170.83	61.30	21.01
Female average	22.67	161.28	52.47	20.17

The experiment is conducted outdoors in spring and autumn, and the environmental conditions at this time are more in line with the actual scene of skateboarding. Temperature: 15 °C± 2 °C, humidity: 60% ± 5%. Each subject filled in the subjective evaluation form before and after the experiment, and scored and evaluated the knee protection, stability, movement flexibility and other indicators of skateboarding pants based on their subjective feelings. The subjective evaluation table is shown in Table 4.

At the beginning of the experiment, the subjects wore their own clothes and sat in the experimental environment for 30 minutes to gradually adapt themselves to the environment. Then, the subjects changed into the designed skateboarding pants, and then filled in part of the questionnaire, including the evaluation of satisfaction with the appearance of skateboarding pants and the convenience of protective gear. After completing part of the questionnaire, the subjects wore ready-made clothes and skated freely for half an hour in the outdoor field. In the process of sports, the subjects can give full play to their skateboarding skills and perform various common movements to simulate the real skateboarding scene. After half an hour of exercise, the subjects immediately filled out the rest of the questionnaire, covering the evaluation of trousers comfort, protector stability, movement flexibility and other aspects. The process of outdoor experiment is shown in Figure 25.

Table 4: Subjective evaluation scale

stage	Evaluation content	Score
Before exercise	Appearance satisfaction	1-10
	Convenience of protective equipment	1-10
After exercise	Pants protection	1-10
	Protector stability	1-10
	Movement flexibility	1-10
	Comfort of protective equipment	1-10
	Sports fatigue	1-10
	Motor performance	1-10

Figure 25: Outdoor experiment process diagram

When studying the performance evaluation of skatewear, the one-way analysis of variance was used to explore the differences between different groups in the eight indicators of appearance satisfaction, convenience of protective gear, pants protection, stability of protective gear, movement flexibility, comfort of protective gear, sports fatigue and sports performance. The analysis results are shown in Table 5. From the significance level, there are significant differences in appearance satisfaction, trousers protection and sports performance between groups ($p < 0.05$), indicating that there are significant differences in these indicators among different groups.

In terms of appearance satisfaction, the average value was 6.18 when wearing protective gear and 8.23 when wearing protective gear. After wearing protective gear, the score increased significantly, indicating that the design of protective gear not only did not damage the appearance beauty of skateboard pants, but may enhance the overall sense of fashion due to Panda elements and other designs; The average score of the convenience of the protective device was 7.88, indicating the convenience of the removable protective device in the wearing operation and improving the convenience of use. After exercise, the average value of trousers' protective property without protective gear was 1.83, and the average value with protective gear was 7.75, the difference was significant, which verified that the protective gear could effectively play a protective role in the scene of skateboard falling, and enhanced the sense of security during exercise; The average score of the stability of protective equipment is 6.75, which is at the upper middle level. It can be further optimized in the future. There was no significant difference in movement flexibility, comfort of protective gear and sports fatigue, indicating that the introduction of protective gear structure did not have a significant impact on human movement flexibility and wearing comfort, and did not increase the additional fatigue burden. The average sports performance was 6.18 without protective gear and 7.18 with protective gear, which was significantly improved after wearing protective gear, indicating that protective gear did not significantly limit the flexibility of skateboard movement while ensuring protection, and even the sense of security brought by protection helped skateboarders to play their sports performance more freely.

To sum up, the designed protective skateboarding pants perform well in terms of appearance and stability of protective equipment. The protective equipment has the advantages of convenience and fall resistance, and has little impact on Sports flexibility, comfort and performance. The overall height meets the actual sports needs of skateboarders.

4 Conclusion

In this study, based on the THUMS human model, the finite element method was used to construct the knee joint fall model of skateboarding, and the stress distribution characteristics of the knee joint under the impact velocity of 1–5 m/s were quantitatively presented. Through the simulation and comparison of Poron, EVA and P4U buffer materials, it is clear that EVA material has the best protection performance. Finally, the stress attenuation law of EVA material with a thickness gradient of 3–15 mm is analyzed, and it is found that 9–12 mm is the optimal thickness range for EVA material to give consideration to protection and comfort. The drop weight impact test further verifies that EVA material has better energy absorption capacity in the actual impact scenario. Finally, we successfully developed a protective skateboard pants that can effectively reduce the risk of sports injury and meet the aesthetic needs of teenagers.

In view of the limitations of objective conditions, as well as the author's lack of time and research level, the research content of this paper still needs to be modified and improved. Future research can be further promoted from the following aspects: First, continue to optimize the finite element model. On the one hand, more individual difference data of human biomechanical parameters are included, so that the model can

Table 5: One way ANOVA

index	Score	F value	P value
Appearance satisfaction			
Wear protective equipment	8.23 ± 1.07	38.60	0.000(*)
Without protective equipment	6.18 ± 1.02		
Convenience of protective equipment	7.88 ± 0.81	/	/
Pants protection			
Wear protective equipment	7.75 ± 0.66	609.49	0.000(*)
Without protective equipment	1.83 ± 0.85		
Protector stability	6.75 ± 1.07	/	/
Movement flexibility			
Wear protective equipment	7.33 ± 0.95	3.03	0.090
Without protective equipment	8.05 ± 1.15		
Comfort of protective equipment			
Wear protective equipment	6.98 ± 0.72	1.04	0.313
Without protective equipment	7.2 ± 0.68		
Sports fatigue			
Wear protective equipment	2.63 ± 0.90	0.262	0.612
Without protective equipment	2.45 ± 1.23		
Motor performance			
Wear protective equipment	7.18 ± 0.77	13.68	0.001(*)
Without protective equipment	6.18 ± 0.94		

* indicates a significant difference ($p < 0.05$)

more accurately reflect the physiological characteristics of different groups; On the other hand, for the modeling of different buffer materials, more dimensional parameters need to be measured to improve the accuracy of the material model. At the same time, more constraints are added in the environment modeling to enhance the simulation accuracy of complex motion scenes and make the simulation results closer to the real motion situation. Second, deepen the research on the performance of buffer materials. This study focuses on the protective performance of the cushioning material after a single fall, and can further explore the performance change rule of the material under the impact of multiple falls, including the attenuation of its cushioning performance, structural stability, etc., to provide a more comprehensive basis for the durability design of the material.

Funding

This work is supported by International Cooperation Fund of Science and Technology Commission of Shanghai Municipality (Grant NO. 2113075010)

Author Contributions

Conceptualization, Yue Ni and Zhaohui Wang; methodology, Yue Ni and Zhaohui Wang; software, Yue Ni; validation, Yue Ni; formal analysis, Yue Ni; investigation, Yue Ni; resources, Zhaohui Wang; data curation, Yue Ni; writing-original draft preparation, Yue Ni; writing-review and editing, Yue Ni and Zhaohui Wang; visualization, Yue Ni; supervision, Zhaohui Wang; project administration, Zhaohui Wang; funding acquisition, Zhaohui Wang. All authors have read and agreed to the published version of the manuscript.

Conflict of Interest

All the authors declare that they have no conflict of interest.

Ethical Approval

Not applicable

References

[1] Shi, F.: Research on sports injury characteristics of adolescent skateboarders. Youth sports **21**(01), 113–114 (2015).

[2] Soligard, T., Palmer, D., Steffen, K., Lopes, A.D., Grek, N., Onishi, K., Shimakawa, T., Grant, M.E., Mountjoy, M., Budgett, R., *et al.*: New sports, COVID-19 and the heat: sports injuries and illnesses in the Tokyo 2020 summer olympics. British Journal of Sports Medicine **57**(1), 46–54 (2023). https://doi.org/10.1136/bjsports-2022-106155

[3] Shuman, K.M., Meyers, M.C.: Skateboarding injuries: An updated review. The Physician and sportsmedicine **43**(3), 317–323 (2015). https://doi.org/10.1080/00913847.2015.1050953

[4] Feletti, F., Brymer, E.: Pediatric and adolescent injury in skateboarding. Research in sports medicine **26**(sup1), 129–149 (2018). https://doi.org/10.1080/15438627.2018.1438285

[5] Yang, S.: Investigation on sports injuries and prevention and rehabilitation strategies of Hello skateboard Club

enthusiasts. Xinjiang Normal University, Master Thesis (2021)

[6] Li, Y., Li, X.: the training basis and winning essentials of skateboarding "bowl pool" project. Contemporary sports Technology **12**(2), 168–172 (2022)

[7] Tian Yang, Dai Jiansong: The current situation of Chinese skateboard team training based on the Olympic strategy. Chinese sports coaches **28**(2), 42–44 (2020)

[8] Rodríguez-Rivadulla, A., Saavedra-García, M.Á., Arriaza-Loureda, R.: Skateboarding Injuries in Spain: A Web-Based Survey Approach. Orthopaedic Journal of Sports Medicine **8**(3), 1–9 (2020). https://doi.org/10.1177/2325967119884907

[9] Keays, G., Dumas, A.: Longboard and skateboard injuries. Injury-international Journal of The Care of The Injured **45**(8), 1215–1219 (2014). https://doi.org/10.1016/j.injury.2014.03.010

[10] Bandzar, S., Funsch, D.G., Hermansen, R., Gupta, S., Bandzar, A.: Pediatric hoverboard and skateboard injuries. Pediatrics **141**(4), e20171253 (2018). https://doi.org/10.1542/peds.2017-1253

[11] Partiali, B., Oska, S., Barbat, A., Sneij, J., Folbe, A.: Injuries to the head and face from skateboarding: a 10-year analysis from national electronic injury surveillance system hospitals. Journal of Oral and Maxillofacial Surgery **78**(9), 1590–1594 (2020). https://doi.org/10.1016/j.joms.2020.04.039

[12] Majercik, S., Day, S., Stevens, M.H., MacDonald, J.D., Bledsoe, J.: Epidemiology of Traumatic Brain Injury After Small-Wheeled Vehicle Trauma in Utah. Neurosurgery **77**(6), 927–30 (2015). https://doi.org/10.1227/neu.0000000000000957

[13] Seasons, M., Morrongiello, B.A.: Adolescents' perspectives on skateboarding and injury risk: the benefits outweigh the risks. Journal of Pediatric Psychology **48**(9), 768–777 (2023). https://doi.org/10.1093/jpepsy/jsad043

[14] Qiao, F., Xu, B., Ying, B., Zhang, X., Wu, X.: Research on the Dynamics Simulation Model Establishment of Stab-resistant Clothing based on Finite Element Analysis. In Textile Bioengineering and Informatics Symposium Proceedings, pp. 428–435 (2018)

[15] Li, J., Chen, D., Tang, X., Li, H.: On the protective capacity of a safety vest for the thoracic injury caused by falling down. BioMedical Engineering OnLine **18**, 40 (2019). https://doi.org/10.1186/s12938-019-0652-3

[16] Pulungan, M.A., Sutikno, Sani M S M: Analysis of bulletproof vest made from fiber carbon composite and hollow glass microsphere (HGM) in absorbing energy due to projectile impact. In 1st South Aceh International Conference on Engineering and Technology, pp. 012001 (2018). https://doi.org/10.1088/1757-899X/506/1/012001

[17] Liu, D.-S., Chen, Z.-H., Tsai, C.-Y., Ye, R.-J., Yu, K.-T.: Compressive Mechanical Property Analysis of Eva Foam: Its Buffering Effects at Different Impact Velocities. Journal of Mechanics **33**(4), 435–441 (2017). https://doi.org/10.1017/jmech.2016.98

[18] Wu, J., Lu, F., Chen, J., Wang, M.: A One-Dimensional Dynamic Constitutive Modeling of Ethylene Vinyl Acetate (EVA) Foam. Polymers **15**(23), 4514 (2023). https://doi.org/10.3390/polym15234514

[19] Zou, S.: Application and processing of EVA. Modern Plastics Processing and Applications **1998**(04), 46–50 (1998)

[20] Chang, B.P., Kashcheev, A., Veksha, A., Lisak, G., Goei, R., Leong, K.F., Tok, A.l.Y., Lipik, V.: Nanocomposite Foams with Balanced Mechanical Properties and Energy Return from EVA and CNT for the Midsole of Sports Footwear Application. Polymers **15**(4), 948 (2023). https://doi.org/10.3390/polym15040948

[21] Tu, H., Xu, P., Yang, Z., Tang, F., Dong, C., Chen, Y., Cao, W., Huang, C., Guo, Y., Wei, Y.: Effect of shear thickening gel on microstructure and impact resistance of ethylene-vinyl acetate foam. Composite Structures **311**, 116811 (2023). https://doi.org/10.1016/j.compstruct.2023.116811

[22] Chang, B.P., Kurkin, A., Kashcheev, A., Leong, K.F., Tok, A.L.Y., Lipik, V.: Enhancing dynamic impact performance and cushioning of EVA copolymer foams with thermoplastic elastomers. Materials Today Communications **38**, 107888 (2024). https://doi.org/10.1016/j.mtcomm.2023.107888

[23] Yang, L., Liu, R., Chu, Q., Wu, F., Feng, J., Feng, X., Zhang, G.: Application of smart materials in rotary steering while drilling instrument . In Proceedings of the International Petroleum and Petrochemical Technology Conference 2022 & International New Energy and Energy Conservation Technology Conference, pp.268–274 (2022)

[24] Xu, Z.: A P4U rubber plastic composite foaming material and its preparation method and application. Chinese Patent CN201910091927.3, 2019-06-11

[25] Zhang, T., Zhou, L., He, J., Gao, S., Zhou, D., Zhang, W., Bao, G.: A P4U rubber plastic composite foaming material and its preparation method and application. Chinese Patent CN202111064673.X, 2023-09-08

[26] PORON® ShockPad Foam. Available online: https://www.rogerscorp.com/elastomeric-material-solutions/poron-industrial-polyurethanes/poron-shockpad-foam

Accessed 2026-02-15

[27] García, A.C., Durá, J.V., Ramiro, J., Hoyos, J.V., Vera, P.: Dynamic Study of Insole Materials Simulating Real Loads. Foot & Ankle International **15**(6), 311–323 (1994). https://doi.org/10.1177/107110079401500606

[28] Caselli, M.A., Levitz, S.J., Clark, N.C., Lazarus, S., Velez, Z., Venegas, L.: Comparison of Viscoped® and PORON® for Painful Submetatarsal Hyperkeratotic Lesions. Journal of the American Podiatric Medical Association **87**(1), 6–10 (1997). https://doi.org/10.7547/87507315-87-1-6

[29] Faulí, A.C., Andrés, C.L., Rosas, N.P., Fernández, M.J., Parreño, E.M., Barceló, C.O.: Physical Evaluation of Insole Materials Used to Treat the Diabetic Foot. Journal of the American Podiatric Medical Association **98**(3), 229–238 (2008). https://doi.org/10.7547/0980229

[30] Watanabe, I., Furusu, K., Kato, C., Miki, K., Hasegawa, J.: Development of practical and simplified human whole body FEM model. JSAE Review **22**(2), 189–194 (2001). https://doi.org/10.1016/S0389-4304(01)00092-3

[31] Arnoux, P.J., Behr, M., Llari, M., Thollon, L., Brunet, C.: Injury criteria implementation and evaluation in FE models applications to lower limb segments. International Journal of Crashworthiness **13**(6), 653–665 (2008). https://doi.org/10.1080/13588260802305089